THE GLOBAL DYNAMICS OF A RAYLEIGH SYSTEM

MERYEM BELATTAR and JAUME LLIBRE

Communicated by Lucian Beznea

This article focuses on the global dynamics of autonomous Rayleigh differential systems depending on one real parameter. By applying methods and classical results from qualitative theory, we describe the geometric behaviour of solutions in the Poincaré disc and prove that these systems exhibit at most one limit cycle.

AMS 2020 Subject Classification: 34A05, 34C05, 34C07, 34C25, 34C29.

Key words: limit cycles, phase portrait, Poincaré disc, Rayleigh system.

1. INTRODUCTION AND STATEMENT OF THE MAIN RESULTS

Since Poincaré's time, many mathematicians and physicists have shown interest in studying nonlinear differential equations due to their extensive applications in modelling various natural phenomena. The Rayleigh equation with constant coefficients, represented by the second-order linear ordinary differential equation

$$\frac{d^2x}{dt^2} + m\frac{dx}{dt} + l^2x = 0,$$

emerged as part of Lord Rayleigh's work on acoustics, particularly in his monumental book "The Theory of Sound" [18]. Rayleigh sought to understand the propagation of sound waves and the behaviour of oscillating systems. To analyse the effects of frictional forces on these oscillatory systems, he introduced a nonlinear term into equation (1), transforming it into the nonlinear Rayleigh equation

(2)
$$\frac{d^2x}{dt^2} + a\left[1 - \frac{1}{3}\left(\frac{dx}{dt}\right)^2\right]\frac{dx}{dt} + x = 0.$$

This equation can also be expressed equivalently in the phase plane (x,y) as

(3)
$$\frac{dx}{dt} = -y, \qquad \frac{dy}{dt} = x + ay - a\frac{y^3}{3},$$

where a is a real parameter related to frictional forces or damping.

MATH. REPORTS **27(77)** (2025), 3-4, 183–195

doi: 10.59277/mrar.2025.27.77.3.4.183

This system and its corresponding equation have applications in modelling a variety of biological and physical phenomena, from human heart-beat rhythms to electrical circuits and control theory. In the heart, for instance, which maintains a stable rhythm despite external disturbances, non-linear damping plays a crucial role in regulating the rhythm back to a normal state, particularly when heart rate increases during physical activities, through adjustments in neural input and hormonal responses.

In radio transmitters, it is crucial to maintain a stable oscillation at a specific frequency for effective signal transmission. Similarly, in feedback control systems, nonlinear damping helps stabilize oscillations by modifying the system's response to perturbations. This stabilization is essential for systems requiring precise control, such as autopilots in aircraft or robotic arms.

In the human heart, electrical circuits, and various systems in control theory, oscillations are self-sustained, meaning that the system can continue oscillating indefinitely without the need of external periodic forces. This behaviour, which occurs as a limit cycle (an isolated periodic orbit), can be effectively modelled by Rayleigh systems.

The dynamics of these systems are complex and interesting, exhibiting periodic behaviour that can be controlled through nonlinear damping, thereby ensuring system stability. As a result, these types of systems have garnered considerable attention from many researchers. Numerous papers have been published on limit cycles, specifically investigating their existence and approximate solutions using various numerical and theoretical approaches. For instance, see [1,3,4,7,8,10,12,15,19,20,23,24].

Our aim in this research is to investigate the qualitative behaviour of system (3) by classifying its global dynamics in the Poincaré disc using Poincaré compactification. Moreover, we establish that this system admits at most one limit cycle using the Poincaré–Bendixson Theorem and a previous result of Lins, Melo and Pugh [11]. By applying the averaging theory, we prove that this unique limit cycle, which encloses the origin, approaches a circle of radius 2 as $|a| \to 0$.

We notice that the system (3) is invariant under the transformation $(x, y, t, a) \mapsto (x, -y, -t, -a)$. Thus instead of studying system (3) for any value of its parameter a, it is sufficient to investigate it for $a \geq 0$, as every trajectory of the system is symmetric with respect to the x-axis in the phase portrait.

In the following sections, Proposition 1.1 and Theorem 1.2 represent our main results, with their proofs provided in Section 4.

PROPOSITION 1.1. The limit cycle of the Rayleigh system (3) is unique and converges to a circle with a radius of 2 as $|a| \to 0$.

THEOREM 1.2. The topologically equivalent phase portraits of system (3) in the Poincaré disc are shown in Figure 1.

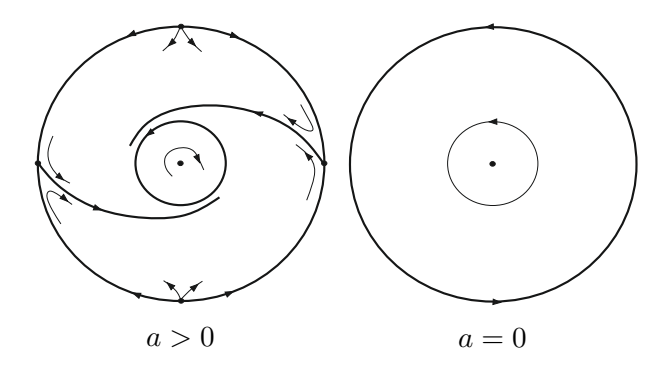


Figure 1 – Phase portraits in the Poincaré disc of the Rayleigh system (3).

The structure of the remainder of this paper is as follows: Section 2 is devoted to the necessary concepts and results required for the proofs of our findings. In Section 3, we determine the local phase portraits at both finite and infinite equilibria.

2. PRELIMINARY RESULTS

2.1. The equilibria

In this section and the following ones, L is defined as the C^{∞} vector field in the plane of degree $n \in \mathbb{N}$ corresponding to the planar nonlinear differential system $(\mathcal{F}, \mathcal{G}) = (\dot{x}, \dot{y})$. Let μ_1 and μ_2 denote the eigenvalues of the linear part $DL(\bar{\mathcal{M}}, \bar{\mathcal{O}})$ where $(\bar{\mathcal{M}}, \bar{\mathcal{O}})$ is an isolated equilibrium of L. Hence,

- (a) $(\bar{\mathcal{M}}, \bar{\mathcal{O}})$ is hyperbolic if μ_1 and μ_2 have non-zero real parts;
- (b) $(\bar{\mathcal{M}}, \bar{\mathcal{O}})$ is semi-hyperbolic if $\mu_1 \mu_2 = 0$ and $\mu_1 + \mu_2 \neq 0$;
- (c) $(\bar{\mathcal{M}}, \bar{\mathcal{O}})$ is nilpotent if $\mu_1 = \mu_2 = 0$ and $DL(\bar{\mathcal{M}}, \bar{\mathcal{O}}) \neq 0$; and
- (d) $(\bar{\mathcal{M}}, \bar{\mathcal{O}})$ is linearly zero if $\mu_1 = \mu_2 = 0$ and $DL(\bar{\mathcal{M}}, \bar{\mathcal{O}}) = 0$.

Equilibrium points of types (a) and (b), known as elementary points, as well as those of type (c), are studied in detail by Dumortier, Llibre, and Artés, including their local phase portraits (see [5, Theorems 2.15, 2.19, and 3.5]).

2.2. The polar blow-up

To characterize the local behaviour of L around a linearly zero singularity, which we assume is located at the origin (0,0), we employ the blow-up method. This technique consists of transforming the singularity into either a circle (polar blow-up) or a line (horizontal and vertical directional blow-ups) through a change of variables. The vector field is then studied in the vicinity of that circle or line. In this section and the following one, we briefly present both the polar and the horizontal blow-ups. For further details, refer to [2] or [5, Chapter 3].

We define the map

$$\Phi:\mathbb{S}^1\times\mathbb{R}_+\to\mathbb{R}^2$$

by $\Phi(\vartheta,\rho)=(x,y)$, where $x=\rho\cos\vartheta,y=\rho\sin\vartheta$, with $\mathbb{R}_+=\{\rho\in\mathbb{R}:\rho\geq0\}$ representing a cylinder. Thus, the generating vector field in $\mathbb{S}^1\times\mathbb{R}_+$, denoted as L_0 , is obtained by the pullback of L, and is expressed as $L_0=D\Phi^{-1}L$. If the m-th Taylor expansion of L at the origin, denoted as $j_m(L(0,0))$, is zero, then it follows that $j_m(L_0(0,0))(w)=0$, for all $w\in\mathbb{S}^1\times\{0\}$. By rescaling time and choosing an appropriate $m\in\mathbb{N}$ such that $j_m(L(0,0))=0$ and $j_{m+1}(L(0,0))\neq0$, we get $\hat{L}_0=\frac{1}{\rho^m}L_0$, whose expression is

$$\dot{\rho} = \frac{x\dot{x} + y\dot{y}}{\rho^{m+1}}, \qquad \ \dot{\vartheta} = \frac{x\dot{y} - y\dot{x}}{\rho^{m+2}}.$$

The behaviour of \hat{L}_0 in the vicinity of the circle $\mathbb{S}^1 \times \{0\}$ (i.e., $\rho = 0$) corresponds to that of L around (0,0).

When a homogeneous polar blow-up is applied more than once, it is called a quasihomogeneous polar blow-up (or (α, β) polar blow-up with $\alpha, \beta \in \mathbb{N}^*$). In this situation, we employ the transformation $\varphi(\vartheta, \rho) = (\rho^{\alpha} \cos \vartheta, \rho^{\beta} \sin \vartheta) = (x, y)$, where the parameters α, β , called weights, are chosen appropriately. The vector field L_0 in $\mathbb{S}^1 \times \mathbb{R}$ is determined similarly. Thus, for a suitable $m \in \mathbb{N}$, we have $L_{\alpha,\beta} = \frac{1}{\rho^m} L_0$ and is written as follows

$$\dot{\rho} = \zeta(\vartheta) \frac{\cos\vartheta \ \rho^{\beta} \dot{x} + \sin\vartheta \ \rho^{\alpha} \dot{y}}{\rho^{\alpha+\beta+m-1}}, \qquad \dot{\vartheta} = \zeta(\vartheta) \frac{\alpha\cos\vartheta \ r^{\alpha} \dot{y} - \beta\sin\vartheta \ \rho^{\beta} \dot{x}}{\rho^{\alpha+\beta+m}},$$

where $\zeta(\vartheta) = (\beta \sin^2 \vartheta + \alpha \cos^2 \vartheta)^{-1}$. Since $\zeta(\vartheta) > 0$, for all $\vartheta \in \mathbb{S}^1$, it becomes possible to eliminate it through a time variable transformation. Therefore, the expression of $L_{\alpha,\beta}$ is

$$\dot{\rho} = \frac{\cos\vartheta \ \rho^{\beta}\dot{x} + \sin\vartheta \ \rho^{\alpha}\dot{y}}{\rho^{\alpha+\beta+m-1}}, \qquad \dot{\vartheta} = \frac{\alpha\cos\vartheta \ \rho^{\alpha}\dot{y} - \beta\sin\vartheta \ \rho^{\beta}\dot{x}}{\rho^{\alpha+\beta+m}}.$$

2.3. The horizontal directional homogeneous blow-up

Consider the origin as a singularity of the system given by

(4)
$$\dot{x} = \mathcal{F}(x,y) = \mathcal{F}_d(x,y) + \cdots, \qquad \dot{y} = \mathcal{G}(x,y) = \mathcal{G}_d(x,y) + \cdots,$$

where \mathcal{F}_d and \mathcal{G}_d are two homogeneous polynomials of degree $d \in \mathbb{N}$. We define the characteristic polynomial function at the origin as

$$V(x,y) = x\mathcal{G}_d(x,y) - y\mathcal{F}_d(x,y).$$

The characteristic directions are given by the straight lines through the origin, which correspond to the real linear factors of the polynomial V. The horizontal blow-up is the variable transformation $(x,y) \mapsto (zy,y)$. Under this transformation, system (4) can be expressed as

(5)
$$\dot{z} = \frac{\mathcal{F}(zy, y) - z\mathcal{G}(zy, y)}{y}, \qquad \dot{y} = \mathcal{G}(zy, y).$$

Therefore, to investigate the dynamics of the original system (4) is equivalent to investigating the new equilibrium points of system (5) that lie on the straight line y = 0. If these equilibrium points on y = 0 remain linearly zero, we repeat this process until they are desingularized.

2.4. The Poincaré compactification

The *Poincaré compactification* is employed to investigate the behaviour of solutions of a planar differential system at infinity. By compactifying the system from the plane \mathbb{R}^2 to the sphere, and extending it analytically to the boundary of this sphere (at infinity), we can establish a link between the local behaviour of each singularity at a finite distance and the behaviour of the system at infinity. This allows us to construct the global phase portrait of the system and consequently determines its global behaviour. For more details, see [9] or [5, Chapter 5]).

We denote the *Poincaré sphere*, the *equator*, the *northern hemisphere*, and the *northern hemisphere* as follows

$$\mathbb{E}^{2} = \{(e_{1}, e_{2}, e_{3}) \in \mathbb{R}^{3} : e_{1}^{2} + e_{2}^{2} + e_{3}^{2} = 1\},$$

$$\mathbb{E}^{1} = \{(e_{1}, e_{2}, e_{3}) \in \mathbb{E}^{2} : e_{3} = 0\},$$

$$M_{+} = \{(e_{1}, e_{2}, e_{3}) \in \mathbb{E}^{2} : e_{3} > 0\},$$

$$M_{-} = \{(e_{1}, e_{2}, e_{3}) \in \mathbb{E}^{2} : e_{3} < 0\},$$

respectively. We identify (w_1, w_2) of \mathbb{R}^2 with $(w_1, w_2, 1)$ in \mathbb{R}^3 and define the central projections $g_+ : \mathbb{R}^2 \to M_+$ as

$$(w_1, w_2) \mapsto g_{\pm}(w_1, w_2) = (e_1, e_2, e_3),$$

where
$$g_{\pm}(w_1, w_2) = \pm \frac{(w_1, w_2, 1)}{\sqrt{w_1^2 + w_2^2 + 1}}$$
.

A straight line connecting the point $(w_1, w_2, 1)$ to the origin of the sphere, intersects the sphere at two points (e_1, e_2, e_3) on M_+ and $(-e_1, -e_2, -e_3)$ on M_- . These projections produce two copies of L, L^+ in M_+ and L^- in M_- , leading to the combined vector field $\mathcal{X}' = \mathcal{X}^+ \cup \mathcal{X}^-$, defined on $\mathbb{E}^2 \backslash \mathbb{E}^1$. By applying the rescaling $e_3^{n-1}\mathcal{X}'$, the vector field \mathcal{X}' is extended from $\mathbb{E}^2 \backslash \mathbb{E}^1$ to \mathbb{E}^2 . The resulting analytic extension is the Poincaré compactified vector field p(L). The projection of M_+ onto $e_3 = 0$ using the transformation $(e_1, e_2, e_3) \mapsto (e_1, e_2)$ is known as the *Poincaré disc* \mathbb{D} . Therefore, the behaviour of p(L) near the equator corresponds to that of L near infinity. The inverse functions of $g_{\pm}(w_1, w_2)$ denoted as $\phi_i : U_i \to \mathbb{R}^2$ and $\psi_i : V_i \to \mathbb{R}^2$, are given by

$$\phi_i(e_1, e_2, e_3) = \psi_i(e_1, e_2, e_3) = \left(\frac{e_m}{e_i}, \frac{e_n}{e_i}\right),$$

for $i \in \{1, 2, 3\}$, where $m \neq i$, $n \neq i$ and m < n. These mappings define three charts of \mathbb{E}^2

$$U_i = \{(e_1, e_2, e_3) \in \mathbb{E}^2 : e_i > 0\} \text{ and } V_i = \{(e_1, e_2, e_3) \in \mathbb{E}^2 : e_i < 0\},\$$

for $i \in \{1, 2, 3\}$. To construct the Poincaré compactified vector field p(L) on the entire sphere, we employ the coordinate (u, v) and the local charts $(U_1, \phi_1), (U_2, \phi_2)$ and (U_3, ϕ_3) . Thus we have

in
$$U_1$$
: $\dot{u} = v^n \left[\mathcal{G}\left(\frac{1}{v}, \frac{u}{v}\right) - u\mathcal{F}\left(\frac{1}{v}, \frac{u}{v}\right) \right], \quad \dot{v} = -v^{n+1}\mathcal{F}\left(\frac{1}{v}, \frac{u}{v}\right),$
in U_2 : $\dot{u} = v^n \left[\mathcal{F}\left(\frac{u}{v}, \frac{1}{v}\right) - u\mathcal{G}\left(\frac{u}{v}, \frac{1}{v}\right) \right], \quad \dot{v} = -v^{n+1}\mathcal{G}\left(\frac{u}{v}, \frac{1}{v}\right),$
in U_3 : $\dot{u} = \mathcal{F}(x, y), \quad \dot{v} = \mathcal{G}(x, y).$

In the local charts V_i , for i = 1, 2, the expression for p(L) is given by $V_i = (-1)^{n-1}U_i$. The points of \mathbb{E}^1 are represented by the coordinate v = 0 in U_i and V_i , i = 1, 2.

To analyse L in \mathbb{R}^2 , including its behaviour at infinity, it is important to study the set $\mathbb{D} = M_+ \cup \mathbb{S}^1$. Hence, for investigating the infinite equilibrium points, it is sufficient to search for these points on $U_1|_{v=0}$, as well as the origin on U_2 . The finite equilibrium points are those on $\mathbb{E}^2 \backslash \mathbb{E}^1$.

The phase portrait of L is represented on the Poincaré disc \mathbb{D} , where its interior, i.e., $\mathbb{D}\backslash\mathbb{E}^1$, contains the finite equilibria of L, while the infinite equilibria are on the equator.

2.5. The Markus-Neumann-Peixoto Theorem

Let p(L) and $p(\mathcal{Y})$ be two Poincaré compactifications on the Poincaré disc \mathbb{D} of the polynomial vector fields L and \mathcal{Y} , respectively, with Φ denoting the flow of p(L).

A trajectory of p(L) that divides the flow into regions, each exhibiting distinct behaviours is called a *separatrix*. This can be either a periodic solution, a singularity, an orbit at infinity, or an orbit on the boundary of a hyperbolic sector of a singularity.

The union of all separatrices of p(L), denoted by S forms a closed set. Each open connected component of $\mathbb{D}\backslash S$ is referred to as a *canonical region* of p(L).

The separatrix configuration of the flow (\mathbb{D}, Φ) is defined as the union of all separatrices \mathcal{S} , along with one selected orbit from each canonical region.

Two separatrix configurations for the flows (\mathbb{D}, Φ) and (\mathbb{D}, Φ^*) are topologically equivalent if there is a homeomorphism of \mathbb{D} that maps the orbits of \mathcal{S}_L to those of \mathcal{S}_L^* while maintaining or reversing the orientation of these orbits.

THEOREM 2.1 (Markus–Neumann–Peixoto Theorem). The phase portraits of p(L) and $p(\mathcal{Y})$ are topologically equivalent if and only if their separatrix configurations are topologically equivalent.

We point the reader to references [6,13,14,16] for the proof of Theorem 2.1.

2.6. The averaging method

We focus on the following two initial value problems:

(6)
$$\dot{y} = \varepsilon G_1(t, y) + \varepsilon^2 G_2(t, y, \varepsilon), \quad y(0) = y_0,$$

and

(7)
$$\dot{z} = \varepsilon g(z), \quad z(0) = y_0,$$

where ε_0 is a small parameter, y, z and $y_0 \in I$, with $I \subset \mathbb{R}^n$ is an open subset. The C^2 -functions $G_1: [0, \infty) \times I \to \mathbb{R}^n$ and $G_2: [0, \infty) \times I \times (0, \varepsilon_0] \to \mathbb{R}^n$ are periodic in the time variable t of period T. The partial derivatives $\frac{\partial G_1}{\partial y}, \frac{\partial^2 G_1}{\partial y^2}$ and $\frac{\partial G_2}{\partial y}$ are bounded and do not depend on ε . We define the averaged function by

(8)
$$g(z) = \frac{1}{T} \int_0^T G_1(t, z) dt.$$

Theorem 2.2. Suppose that $z(t) \in I$ for $t \in [0, 1/\varepsilon]$. Then

- (i) For all $t \in [0, 1/\varepsilon]$, $y(t) z(t) = O(\varepsilon)$ as $\varepsilon \to 0$.
- (ii) If $q \neq 0$ is a singularity of the initial value problem (7), and
- (iii) $\det\left(\frac{\partial g(z)}{\partial z}|_{z=q}\right) \neq 0$, hence the problem (6) has a limit cycle $y(t,\varepsilon)$ of period T such that $y(0,\varepsilon) \to q$ when $\varepsilon \to 0$.

Proof. See Theorem 11.5 of [21]. \Box

2.7. Uniqueness of limit cycle

In this section, we present the uniqueness result of a periodic solution to the Liénard vector field (see [11, Section 2]), which we need for proving Proposition 1.1.

Theorem 2.3. Consider the Liénard vector field of degree three, given by

(9)
$$\mathcal{L}(x,y) = (y - f(x), -x),$$

where $f(x) = a_3x^3 + a_2x^2 + a_1x$. Then

- (1) If $a_1a_3 > 0$, \mathcal{L} has no closed orbits.
- (2) If $a_1a_3 < 0$, there exists a unique closed orbit for \mathcal{L} .
- (3) If $a_1 = 0$ and $a_3 \neq 0$, \mathcal{L} has no closed orbits. The origin is a weak attractor for $a_3 > 0$ and a weak repeller for $a_3 < 0$.
- (4) If $a_1 \neq 0$ and $a_3 = 0$, \mathcal{L} has no closed orbits. The origin is hyperbolic attractor for $a_1 > 0$ and a hyperbolic repeller for $a_1 < 0$.
 - (5) If $a_1 = a_3 = 0$, the origin is classified as a centre.

3. LOCAL PHASE PORTRAITS OF THE EQUILIBRIA

In order to characterize the phase portraits of system (3), we first investigate all the equilibria and their local behaviours.

3.1. Finite equilibria

PROPOSITION 3.1. At a finite distance, the differential system (3) with $a \ge 0$ admits the origin O(0,0) as its only trivial singularity. The corresponding local phase portrait is

- (1) a hyperbolic unstable focus for 0 < a < 2;
- (2) a hyperbolic unstable node for $a \ge 2$;
- (3) a center if a = 0.

Proof. When $a \ge 0$, system (3) possesses only one singularity, the origin (0,0), whose eigenvalues are $(a \pm \sqrt{a^2 - 4})/2$. Hence, (0,0) is classified as a hyperbolic unstable focus when 0 < a < 2; and as a hyperbolic unstable node when $a \ge 2$.

If a=0 system (3) can be written as $\dot{x}=-y,\quad \dot{y}=x,$ with the eigenvalues $\pm i$ at (0,0). So it is a centre. \Box

3.2. Infinite equilibria

PROPOSITION 3.2. At infinity, the differential system (3) exhibits the following behaviours:

- (a) in U_1 , the origin is a linearly zero equilibrium for a > 0, with a local phase portrait consisting of four hyperbolic sectors. When a = 0, no equilibria exist;
- (b) in U_2 , the origin is classified as a hyperbolic unstable node for a > 0, and is not an equilibrium when a = 0.

Proof. The system (3) in U_1 is expressed as follows:

(10)
$$\dot{u} = \frac{du}{dt} = -\frac{a}{3}u^3 + v^2 + auv^2 + u^2v^2, \qquad \dot{v} = \frac{dv}{dt} = uv^3.$$

If $a \neq 0$, we observe that system (10) has the solution v = 0. Thus $\dot{u}|_{v=0} = -\frac{a}{3}u^3$. Consequently system (10) possesses the origin as its unique equilibrium, and this point is a linearly zero. To investigate its local phase portrait, we first use a (2,3) polar blow-up, and after a horizontal directional quasihomogeneous blow-up. Thus, by applying the transformation $(u,v) \mapsto (\rho^2 \cos \vartheta, \rho^3 \sin \vartheta)$, we get

$$\dot{\rho} = \frac{1}{3}\rho^5 \cos \vartheta (-a\cos^3 \vartheta + 3a\rho^2 \cos \vartheta \sin^2 \vartheta + 3\rho^4 \cos^2 \vartheta \sin^2 \vartheta + 3\sin^2 \vartheta + 3\rho^4 \sin^4 \vartheta)$$
(11)
$$+ 3\rho^4 \sin^4 \vartheta)$$

$$\dot{\vartheta} = -\rho^4 \sin \vartheta (-a \cos^3 \vartheta + 3a\rho^2 \cos \vartheta \sin^2 \vartheta + \rho^4 \cos \vartheta^2 \sin^2 \vartheta + 3\sin^2 \vartheta).$$

After the time rescaling $ds = \rho^4 dt$, system (11) becomes

(12)
$$\dot{\rho} = -\frac{a}{3}\rho\cos^4\vartheta + a\rho^3\cos^2\vartheta\sin^2\vartheta + \rho^5\cos^3\vartheta\sin^2\vartheta + \cos\vartheta(\rho\sin^2\vartheta + \rho^5\sin^4\vartheta),$$
$$\dot{\vartheta} = a\cos^3\vartheta\sin\vartheta - 3a\rho^2\cos\vartheta\sin^3\vartheta - \rho^4\cos^2\vartheta\sin^3\vartheta - 3\sin^3\vartheta.$$

The system (12) has two equilibria on the circle $\rho = 0$: the origin (0,0) and the point (0, π), both of which are saddles with eigenvalues -a/3 and a at each.

Now, we perform the horizontal directional quasihomogeneous blow-up using the transformation $(u, v) \mapsto (u_1 v_1^2, v_1^3)$. Thus we obtain

(13)
$$\dot{u} = \frac{1}{3}v_1^4(3 - au_1^3 + 3au_1v_1^2 + u_1^2v_1^4), \qquad \dot{v} = \frac{1}{3}u_1v_1^9.$$

Taking into account the time rescaling $ds = v_1^4 dt$, the new differential system is given by

(14)
$$\dot{u} = \frac{1}{3}(3 - au_1^3 + 3au_1v_1^2 + u_1^2v_1^4), \qquad \dot{v} = \frac{1}{3}u_1v_1^5.$$

At $v_1 = 0$, the point $(\sqrt[3]{3/a}, 0)$ is the only equilibrium of system (14). Since the eigenvalues of the linear part of (14) at this point are $-\sqrt[3]{9a}$ and 0, it is a semi-hyperbolic equilibrium point. After translating this point to the origin via the variable substitution $u_1 = u_2 + \sqrt[3]{3/a}$ and applying Theorem 2.19 of [5], we find that the local phase portrait at the origin consists of four hyperbolic sectors as represented in Figure 2.

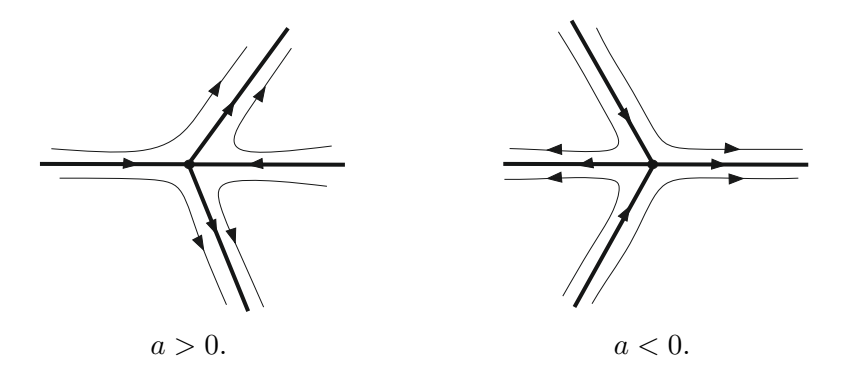


Figure 2 – The Blow-up of the origin of the local chart U_1 when $a \neq 0$.

The polynomial differential system (3) in U_2 reads

(15)
$$\dot{u} = \frac{1}{3}au - v^2 - auv^2 - u^2v^2, \qquad \dot{v} = \frac{1}{3}av - av^3 - uv^3.$$

For $a \neq 0$, we have $\dot{u}|_{v=0} = \frac{1}{3}au$. Obviously, the origin is the only singularity of system (15), whose Jacobian matrix has a double eigenvalue of a/3. Thus, for a > 0, the origin is an unstable node.

When a=0, no singularity exists in U_1 , since $\dot{u}|_{v=0}=1+u^2\neq 0$. Similarly, the origin is not an equilibrium point in U_2 as $\dot{u}|_{v=0}=-1-u^2\neq 0$. Therefore, system (10) has no equilibrium points at infinity. \square

4. PROOF OF PROPOSITION 1.1 AND THEOREM 1.2

We first show that system (3) possesses no more than one limit cycle.

From the phase portrait of the infinite equilibrium points, as shown in Figure 1 for a>0, we see that infinity is a repeller, i.e., inside the Poincaré disc there are no trajectories ending at infinity. Inside the Poincaré disc, the only equilibrium point is the origin, which is also a repeller. Thus, based on the Poincaré–Bendixson Theorem (see [17] or [22]), any orbit inside the Poincaré disc of system (3) apart from the origin cannot tend in forward time to a singularity, and consequently to a graphics, then it must tend toward the periodic orbit of the system. Thus, at least one limit cycle exists in the interior of the Poincaré disc \mathbb{D} , enclosing the focus at the origin.

Moreover, by applying the transformation $(x, y) \mapsto (y, x)$ to system (3), we obtain the Liénard system of degree three (9) where $a_1 = a, a_2 = 0$ and $a_3 = -a/3$. According to statement (2) of Theorem 2.3, we conclude that the limit cycle of system (3), when it occurs, is unique.

Now we show that this periodic orbit, enclosing the origin, approaches the circle of radius 2 as $|a| \to 0$. Indeed, using the polar coordinate transformations $x = \rho \cos \vartheta$ and $y = \rho \sin \vartheta$, system (3) takes the form

(16)
$$\dot{\rho} = a\rho \sin^2 \vartheta - \frac{1}{3}a\rho^3 \sin^4 \vartheta, \qquad \dot{\vartheta} = 1 + a\cos\vartheta\sin\vartheta - \frac{1}{3}a\rho^2\cos\vartheta\sin^3\vartheta.$$

In terms of the new variable ϑ , system (16) leads to the differential equation

(17)
$$\frac{d\rho}{d\vartheta} = \frac{3a\rho\sin^2\vartheta - a\rho^3\sin^4\vartheta}{3 + 3a\cos\vartheta\sin\vartheta - a\rho^2\cos\vartheta\sin^3\vartheta}.$$

For a > 0 sufficiently small, we develop the right-hand side of equation (17) into a power series with respect to this parameter a. Thus we get

(18)
$$\frac{d\rho}{d\vartheta} = a(\rho \sin^2 \vartheta - \frac{1}{3}\rho^3 \sin^4 \vartheta) + O(a^2) = aG_1(\vartheta, \rho) + O(a^2).$$

Integrating equation (8) with respect to ϑ from 0 to $T=2\pi$, the first averaged function is

(19)
$$g(\rho) = -\frac{1}{8}\rho(\rho^2 - 4).$$

Equation (19) has a unique positive real solution for the variable ρ , which is $\rho = 2$ with $g'(2) = -1 \neq 0$. Therefore, system (3) has a periodic solution $\rho(\vartheta, a)$ of period 2π , which approaches the circle of radius 2 when $a \to 0$.

In summary, Proposition 1.1 and Theorem 1.2 are proved.

5. CONCLUSION

In this study, we have successfully identified the global dynamics of a class of planar autonomous Rayleigh differential systems. We have characterized the global phase portraits of the system by analysing the local behaviour of all its equilibria in the Poincaré disc. Our analysis revealed that there is at least one limit cycle surrounding a focus at the origin. Furthermore, through a straightforward change of variables, we have established that this limit cycle is unique.

Finally, we have analytically determined the limit cycle using the averaging method. This limit cycle, denoted as $\rho(\vartheta,a)$, has a period of 2π and a radius $\rho=2$, provided a>0 is sufficiently small.

Acknowledgments. Jaume Llibre is partially supported by the Agencia Estatal de Investigación of Spain (Grant no. PID2022-136613NB-100), AGAUR-Generalitat de Catalunya (Grant no. 2021SGR00113), and by the Reial Acadèmia de Ciències i Arts de Barcelona.

REFERENCES

- [1] M.A. Abdelkader, Exact solutions for Rayleigh's equation with variable mass. J. Natur. Sci. Math. 21 (1981), 1, 63–79.
- [2] M.J. Álvarez, A. Ferragut, and J. Xavier, A survey on the blow up technique. Internat.
 J. Bifur. Chaos Appl. Sci. Engrg. 21 (2011), 11, 3103-3118.
- [3] M.D. Baldissera, J. Llibre, and R. Oliveira, *Dynamics of a generalized Rayleigh system*. Differ. Equ. Dyn. Syst. **32** (2024), *3*, 933–941.
- [4] P. Băzăvan, The limit cycle of the unforced Rayleigh system. An. Univ. Craiova Ser. Mat. Inform. **30** (2003), 40–47.
- [5] F. Dumortier, J. Llibre, and J.C. Artés, Qualitative theory of planar differential systems. Universitext, Springer, Berlin, 2006.
- [6] J.G. Espín Buendía and V. Jiménez López, On the Markus-Neumann theorem. J. Differential Equations 265 (2018), 11, 6036-6047.
- [7] A. Georgescu, P. Băzăvan, and M. Sterpu, Approximate limit cycles for the Rayleigh model. ROMAI J. 4 (2008), 2, 73–80.
- [8] A. Ghaffari, On Rayleigh's nonlinear vibration equation, In: Qualitative Methods in the Theory of Non-Linear Vibrations (Proc. Internat. Sympos. Non-Linear Vibrations, 1961), pp. 131–133. Izdat. Akad. Nauk Ukrain. SSR, Kiev, 1963.
- [9] E.A. González Velasco, Generic properties of polynomial vector fields at infinity. Trans. Amer. Math. Soc. 143 (1969), 201–222.
- [10] A. Grin and K.R. Schneider, Global algebraic Poincaré-Bendixson annulus for the Rayleigh equation. Electron. J. Qual. Theory Differ. Equ. 2023 (2023), article no. 35.
- [11] A. Lins, W. de Melo, and C.C. Pugh, On Liénard's equation. In: Geometry and Topology (Proc. III Latin Amer. School of Math., Rio de Janeiro, 1976), pp. 335–357. Lecture Notes in Math. 597, Springer, Berlin, New York, 1977.

- [12] M.A. López and R. Martínez, A note on the generalized Rayleigh equation: Limit cycles and stability. J. Math. Chem. 51 (2013), 4, 1164–1169.
- [13] L. Markus, Global structure of ordinary differential equations in the plane. Trans. Amer. Math. Soc. 76 (1954), 127–148.
- [14] A.D. Neumann, Classification of continuous flows on 2-manifolds. Proc. Amer. Math. Soc. 48 (1975), 73–81.
- [15] A. Palit and D.P. Datta, Comparative study of homotopy analysis and renormalization group methods on Rayleigh and Van der Pol equations. Differ. Equ. Dyn. Syst. 24 (2016), 4, 417–443.
- [16] M.M. Peixoto, On the classification of flows on 2-manifolds, In: Dynamical Systems (Proc. Sympos., Univ. Bahia, Salvador, 1971), pp. 389–419. Academic Press, New York, London, 1973.
- [17] L. Perko, Differential Equations and Dynamical Systems. Texts Appl. Math. 7, Springer, New York, 1991.
- [18] J. Rayleigh, The Theory of Sound, Second ed. Dover Publications, New York, 1945.
- [19] S. Saha, G. Gangopadhyay, and D.S. Ray, Systematic designing of bi-rhythmic and trirhythmic models in families of Van der Pol and Rayleigh oscillators. Commun. Nonlinear Sci. Numer. Simul. 85 (2020), article no. 105234.
- [20] M. Sterpu, A. Georgescu, and P. Băzăvan, Dynamics generated by the generalized Rayleigh equation II. Periodic solutions. Math. Rep. (Bucur.) 2(52) (2000), 3, 367–378.
- [21] F. Verhulst, Nonlinear Differential Equations and Dynamical Systems. Universitext, Springer, Berlin, 1990.
- [22] S. Wiggins, Introduction to Applied Nonlinear Dynamical Systems and Chaos. Texts Appl. Math. 2, Springer, New York, 1990.
- [23] F. Zanolin, Periodic solutions for differential systems of Rayleigh type. Rend. Istit. Mat. Univ. Trieste 12 (1980), 1-2, 69-77.
- [24] E.D. Žitel'zeĭf, The limit cycles of the Rayleigh equation. Differ. Uravn. 8 (1972), 7, 1309–1311.

Received 14 October 2024

Meryem Belattar
Laboratory of Applied Mathematics,
Department of Mathematics, Faculty of Sciences,
Ferhat Abbas University-Sétif 1,
P.O. Box 19 000, Sétif, Algeria
meryem.belattar2019@gmail.com

Jaume Llibre
Departament de Matemàtiques,
Universitat Autònoma de Barcelona,
08193 Bellaterra, Barcelona, Catalonia, Spain
jaume.llibre@uab.cat